



Leaching kinetics of antimony-bearing complex sulfides ore in hydrochloric acid solution with ozone

Xue-yi GUO^{1,2}, Yun-tao XIN^{1,2}, Hao WANG^{1,2}, Qing-hua TIAN^{1,2}

1. School of Metallurgy and Environment, Central South University, Changsha 410083, China;

2. Cleaner Metallurgical Engineering Research Center,
China Nonferrous Metals Industry Association, Changsha 410083, China

Received 30 June 2016; accepted 23 February 2017

Abstract: The leaching kinetics of Sb and Fe from antimony-bearing complex sulfides ore was investigated in HCl solution by oxidation–leaching with ozone. The effects of temperature, HCl concentration, stirring speed and particle size on the process were explored. It is found that the recoveries of Sb and Fe reach 86.1% and 28.8%, respectively, when the reaction conditions are 4.0 mol/L HCl, 900 r/min stirring speed at 85 °C with <0.074 mm particle size after 50 min leaching. XRD analysis indicates that no new solid product forms in the leaching residue and the leaching process can be described by shrinking core model. The leaching of Sb corresponds to diffusion-controlled model at low temperature (15–45 °C) and mixed-controlled model at high temperature (45–85 °C), and the apparent activation energies are 6.91 and 17.93 kJ/mol, respectively. The leaching of Fe corresponds to diffusion-controlled model, and the apparent activation energy is 1.99 kJ/mol. Three semi-empirical rate equations are obtained to describe the leaching process.

Key words: ozone; antimony-bearing complex sulfides ore; oxidation–leaching kinetic; mixed-controlled model; diffusion-controlled model

1 Introduction

Most antimony is usually used as flame retardants, catalysts in plastics production, pigments in paints and in production of glassware [1]. China is the largest producer of antimony in the world [2]. The most important antimony resource exploited in China is the antimony ore containing stibnite (Sb_2S_3). Traditionally, extraction of antimony from stibnite involves a two-step pyrometallurgical process including roasting and carbothermal reduction [3,4]. However, the pyrometallurgical process usually results in serious environmental pollution and high energy consumption [5].

Compared with the pyrometallurgy technology, the hydrometallurgical process is considered as an environmental friendly technique which has attracted much attention due to its potentials in dealing with low grade complex stibnite [6]. Leaching of stibnite in an alkaline solution was proposed by previous

researchers [7–10] and has been employed industrially in China, Australia and United States. In the acidic chloride system, hydrochloric acid was used as the lixiviant in conjunction with oxidants, such as ferric chloride, chlorine and antimony pentachloride for antimony recovery from stibnite [11–13].

In our previous research [14,15], the extraction of antimony from complex sulfides ore was studied and the optimized conditions were obtained. However, few research has been reported on the kinetics of antimony leaching by ozone. In this work, the kinetics of antimony and iron from complex sulfides ore and the factors affecting antimony extraction were investigated.

2 Experimental

2.1 Materials

The composition and phases of ore are reported in our previous study [14]. In the experiments, the ore was crushed to sizes of <0.074, 0.074–0.089, 0.089–0.124

and 0.124–0.179 mm. The concentration of metal element in this ore was determined by inductively coupled plasma atomic emission spectrometry (ICP-AES, PS-6, Baird, USA) and X-ray fluorescence (XRF, S0902724, Rigaku, Japan). The mineralogical composition was identified by X-ray diffractometry (XRD, S0902240, Rigaku, Japan). At the same time, the antimony and iron in leaching solution were analyzed by ICP-AES for kinetics analysis.

Analytical grade hydrochloric acid (36%–38%, mass fraction) was used to prepare the HCl solutions. Industrial grade oxygen was used to produce ozone for the leaching process and the mass flow of the ozone controlled by an ozonizer (OZOMJB–80B, ANQIU OZOMAX EQUIPMENT, China) was 120 mg/L.

2.2 Leaching procedure

The leaching experiments were carried out in the same way as our previous study [14], except the liquid to solid ratio.

The 400 mL of HCl solution of required mole ratio diluted with water was added to the beaker. When the temperature reached the set value, 8.0 g of the antimony-bearing complex sulfides ore was added, and the ozone gas was pumped into the solution. A condenser was used to prevent evaporation during the experiment. 5.0 mL of the liquid sample was collected and tested by ICP-AES every 10 min, and at the same time, 5.0 mL of the HCl solution was added to the system to keep the solution volume unchanged. After 50 min leaching process, the slurry was withdrawn from the reactor by vacuum filtered. The residue was sent to detect after drying in oven. The volume of the filtered pregnant solution was measured by a measuring cylinder. The leaching efficiency is calculated based on the sampling solutions in pre-determined intervals and the leaching efficiency of antimony (or iron), x , is defined by

$$x = cV / (m\omega) \quad (1)$$

where c , V , m and ω are the antimony concentration in filtration, the volume (we assumed it as constant), mass and antimony (or iron) content, respectively. The effects of temperature, acid concentration, stirring speed and particle size on the leaching process were investigated.

3 Results and discussion

3.1 Leaching behavior and kinetics model of antimony

3.1.1 Effects of temperature on leaching efficiency of antimony

Figure 1 shows the effect of temperature on the leaching efficiency of antimony in the range of 15–85 °C. The operating conditions are 4.0 mol/L HCl, 900 r/min

stirring speed, 2.0 L/min gas flow rate, <0.074 mm particle size and 50 mL/g L/S ratio. The results indicate that the leaching efficiency of antimony increases with the increase of temperature and the leaching efficiency of Sb rises from 19.9% at 15 °C to 86.1% at 85 °C. This is because the mass transfer between ore, ozone gas and lixivium is promoted with the increase of temperature, and the reactions could happen more easily at high temperature.

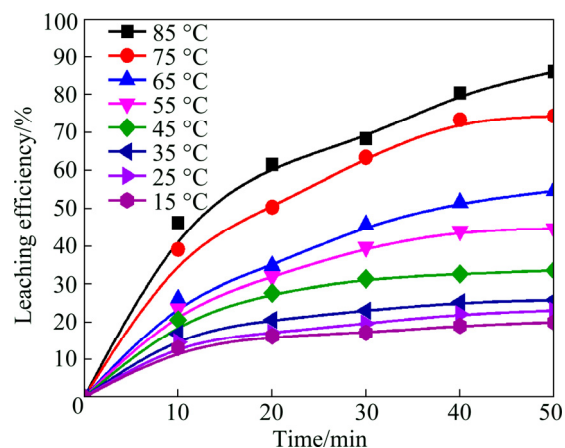


Fig. 1 Effects of temperature on leaching efficiency of antimony from antimony-bearing complex sulfides ore

According to XRD pattern of leaching residue, no sulfur was found in the leaching residue [14], meaning that the sulfur in ore was transformed into sulfate instead of elemental sulfur. There is no solid product generated in the leaching process and the leaching process can be described as typical shrinking core model [16,17]. The empirical equations are listed below:

$$1 - (1-x)^{1/3} = k_1 t \quad (2)$$

$$1 - (1-x)^{2/3} = k_2 t \quad (3)$$

$$1 - (1-x)^{1/3} + \beta [1 - (1-x)^{2/3}] = k_3 t \quad (4)$$

$$\beta = k_1 / k_2$$

where Eq. (2) shows chemical reaction control, Eq. (3) is mass-diffusion control and Eq. (4) stands for mixed-control, x stands for leaching efficiency, k_i is rate constants and t is reaction time.

In order to determine the kinetic parameters and rate-controlling step of antimony leaching process, the experimental data presented in Fig. 2 is fitted by Eqs. (2)–(4). The linear relative coefficients of plots of Eqs. (3) and (4) vs time are higher than that of Eq. (2), indicating that the diffusion control and mixed control model are suitable for the leaching process. The plots are shown in Fig. 2, where the k_2 and k_3 could be obtained. According to Arrhenius equation, it is represented as

$$k=A\exp[-E/(RT)] \tag{5}$$

$$\ln k=\ln A-[E/(RT)] \tag{6}$$

where A is the pre-exponential factor; R stands for the mole gas constant; T is the thermodynamic temperature; E is the apparent activation energy.

From the k obtained from Fig. 2, the rate constants (k , min^{-1}) are determined and plotted against $1/T$ (Arrhenius plot), as presented in Fig. 3. From Fig. 3, it is easily seen that the plots fit two different lines at high temperature (45–85 °C) and low temperature (15–45 °C), respectively. The plot at high temperature has larger slope than that of low temperature, which means the higher activation energy, so k value at high temperature is obtained with data fitted by Eq. (4) and k value at low temperature is obtained with data fitted by Eq. (3).

As shown in Fig. 3, the calculated apparent activation energy is 17.93 kJ/mol at 45–85 °C and 6.91 kJ/mol at 15–25 °C. Usually, the activation energy of diffusion controlled process is less than 10 kJ/mol, while the value is greater than 40 kJ/mol for a chemically controlled process, so the activation energy of mixed controlled process is between 10 and 40 kJ/mol [18]. Therefore, the activation energy indicates that the

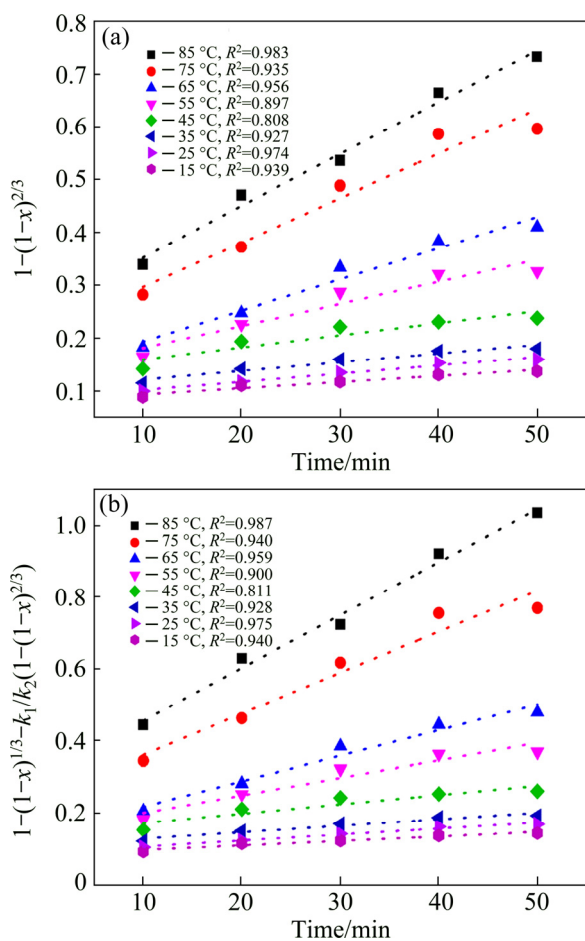


Fig. 2 Plots of $1-(1-x)^{2/3}$ vs time (a) and $1-(1-x)^{1/3}+k_1/k_2(1-(1-x)^{2/3})$ vs time (b) at different reaction temperatures

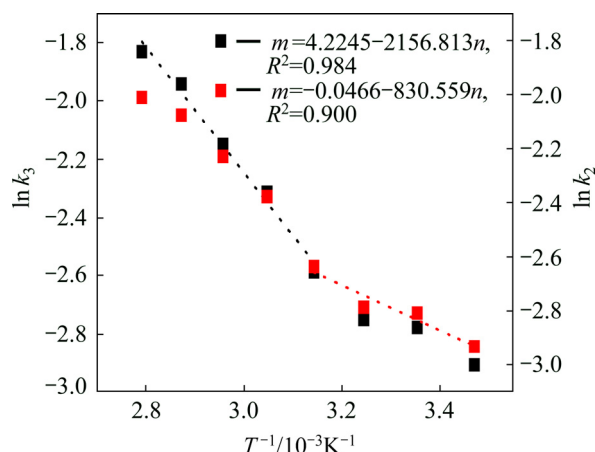


Fig. 3 Arrhenius plot for antimony leaching from complex sulfides ore

antimony leaching process from complex sulfides ore belongs to mixed controlling process at high temperature and mass diffusion at low temperature.

3.1.2 Effect of acid concentration, stirring speed, particle size and kinetic model at high temperature

In order to figure out the kinetic model at high temperature, the effects of acid concentration, stirring speed and particle size were investigated, respectively.

Figure 4(a) shows the result of antimony extraction in the range of 2.0–5.0 mol/L HCl. The extraction of antimony increases significantly from 41.7% to 61.9% with the increase of hydrochloric acid concentrations from 2.0 to 5.0 mol/L. It is well known that the antimony is in the form of SbCl_x complex in the hydrochloric acid solution and the Cl^- could enhance the stability and solubility of antimony because of the complexation [4,19], so the leaching efficiency of antimony increases with the increase of HCl concentration and the leaching efficiency quickly achieves the equilibrium at 30 min with 5.0 mol/L HCl. Figure 4(b) shows the result of antimony extraction with the stirring speed of 300–900 r/min. This leaching process involves gas–liquid–solid three phase reaction. The stirring speed mainly affects mass transfer, and high stirring speed enhances the interface behavior of reactants and promotes the leaching process. Figure 4(c) presenting the effect of particle size shows that the leaching efficiency of antimony increases slightly with the decrease of particle size. The results indicate that the smaller particle has the larger specific surface area and promotes the mass transfer process at the gas–solid–liquid interface.

The rate constant k is related to the acid concentration, stirring speed and particle size which could be seen from Figs. 4(d), (e) and (f). The dependence of the rate constant on these variables can be expressed with the Arrhenius equation:

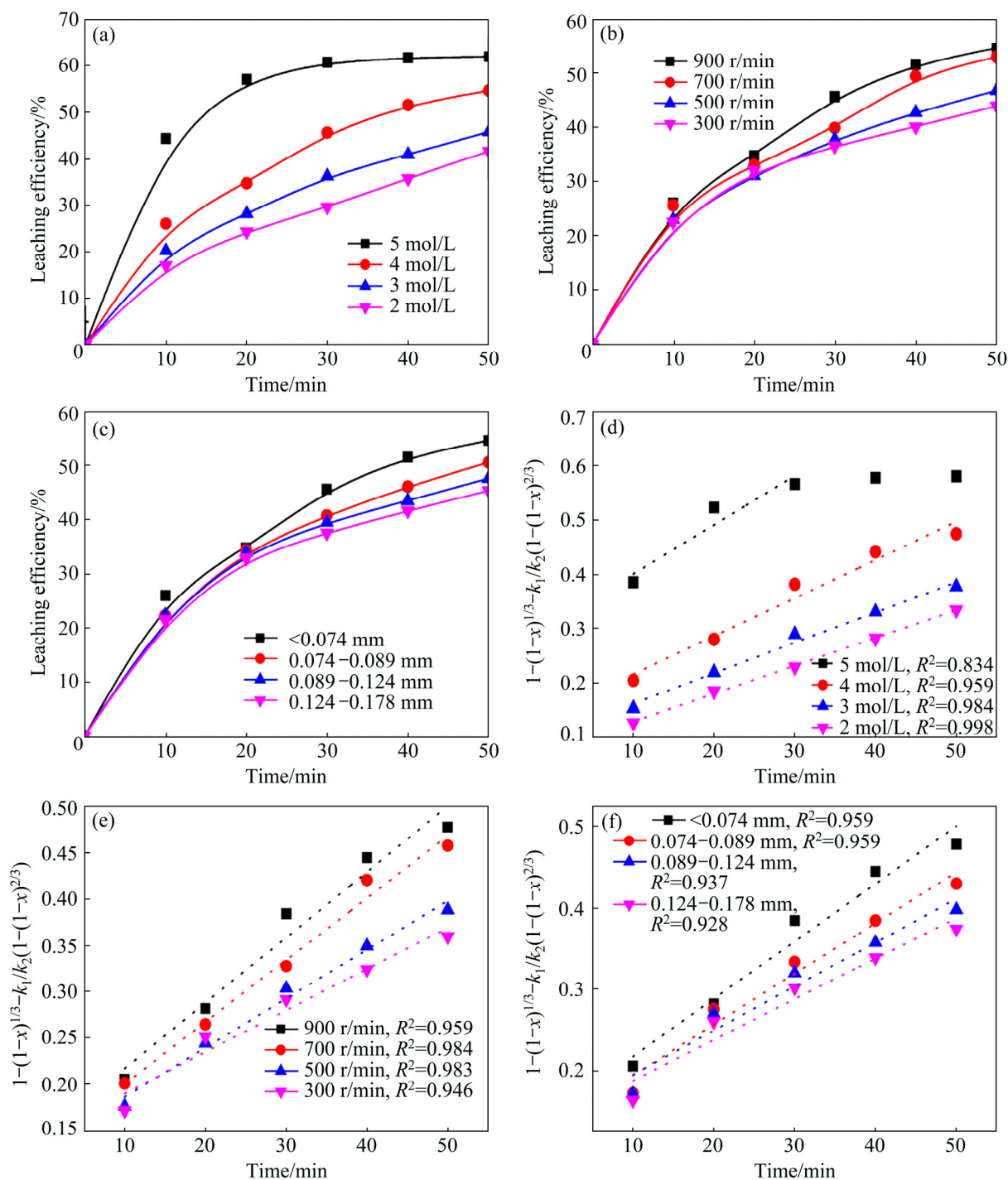


Fig. 4 Leaching efficiency of antimony at 65 °C and plots of $1-(1-x)^{1/3}+k_1/k_2(1-(1-x)^{2/3})$ vs time

$$k=A_0C^aS^b d^c \exp[-E_a/(RT)] \tag{7}$$

where A_0 is the frequency factor; E_a is the apparent activation energy; C is the hydrochloric acid concentration; S is the stirring speed, d is the particle size; a , b and c are the constants.

The slopes of the lines in Figs. 4(d), (e) and (f) represent the rate constant k . The $\ln k$ can be calculated from the k value. The values of a , b and c in Eq. (7) are determined by linear regression analysis according to $\ln k$, $\ln C$, $\ln S$ and $\ln d$, respectively (Table 1), to be

$a=0.6030$, $b=0.4405$ and $c=-0.3896$, so the pre-exponential factor in Eq. (5) becomes

$$A=A_0C^{0.6030}S^{0.4405}d^{-0.3896} \tag{8}$$

Table 1 Fitting results of $\ln k_3$ vs $\ln C$, $\ln S$ and $\ln d$

Factor	Linear equation	R^2
HCl concentration	$m=0.6030n-5.7523$	0.848
Stirring speed	$m=0.4405n-7.9339$	0.955
Particle size	$m=-0.3896n-5.9966$	0.928

The intercept of line in Fig. 3 is $\ln A$, and A value is 68.34. Based on Eq. (8), the value of A_0 is determined to be 20.95 s^{-1} . Above all, we can get the leaching kinetics equation at high temperature:

$$1-(1-x)^{1/3}-k_1/k_2(1-(1-x)^{2/3})=20.95C^{0.6030}S^{0.4405}d^{-0.3892}\exp(-17931.75/(RT))t \quad (9)$$

3.1.3 Effect of acid concentration, stirring speed and particle size and kinetic model at low temperature

The kinetic model at low temperature was also studied. The operating conditions at 25°C were the same as those at 65°C , and the results are presented in Fig. 5.

From Figs. 5(a), (b) and (c), it is easily seen that the leaching efficiency of antimony increases with the increase of HCl concentration and stirring speed and the decrease of particle size. This is because the mass transfer at 25°C is promoted by increasing HCl concentration and stirring speed. And the smaller particle has larger specific surface area, so the leaching process is enhanced. Based on the conclusion obtained by temperature experiment, the data are fitted by Eq. (3), and the results are well fitted by the diffusion controlled process, as shown in Figs. 5(d), (e) and (f).

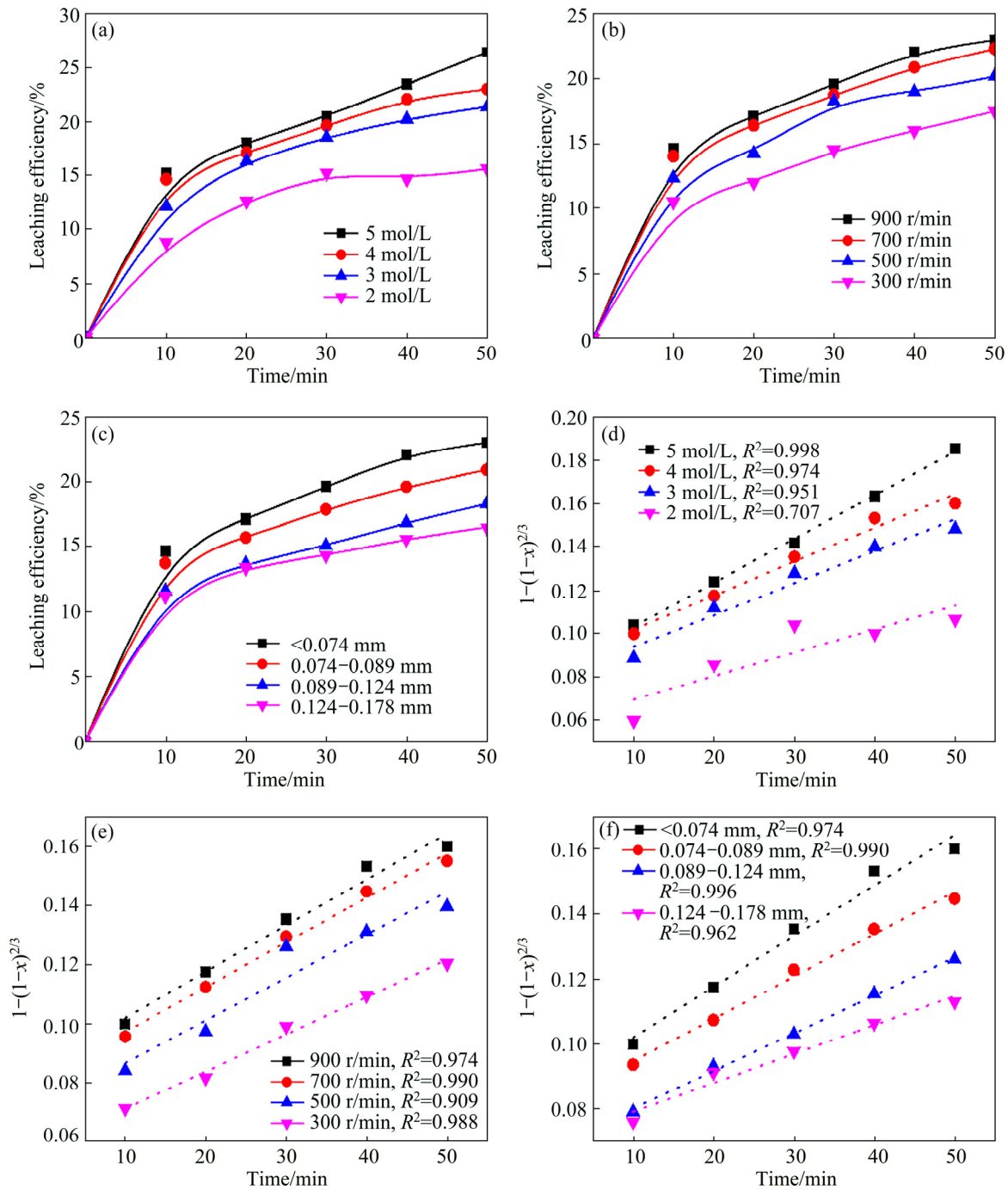


Fig. 5 Leaching efficiency of antimony at 25°C and plots of $1-(1-x)^{2/3}$ vs time

The slopes of the lines in Figs. 5(d), (e) and (f) represent the rate constant. The $\ln k$ can be calculated from the k value. The values of a , b and c in Eq. (7) are determined by linear regression analysis according to $\ln k$, $\ln C$, $\ln S$ and $\ln d$, respectively (Table 2), to be $a=0.6242$, $b=0.1937$, $c=-0.5957$, so the pre-exponential factor in Eq. (5) becomes

$$A=A_0C^{0.6242}S^{0.1937}d^{-0.5957} \quad (10)$$

The intercept of line in Fig. 3 is $\ln A$, and A value is 0.9545. Based on Eq. (10), the value of A_0 is determined to be 6.19 s^{-1} . Above all, we can get the leaching kinetics equation at low temperature:

$$1-(1-x)^{2/3}=6.19C^{0.6242}S^{0.1937}d^{-0.5957}\exp(-6905.3/(RT))t \quad (11)$$

Table 2 Fitting results of $\ln k_3$ vs $\ln C$, $\ln S$ and $\ln d$

Factor	Linear equation	R^2
HCl concentration	$m=0.6242n-7.2500$	0.925
Stirring speed	$m=0.1937n-7.7667$	0.936
Particle size	$m=-0.5957n-8.0380$	0.961

3.2 Leaching behavior and kinetics model of iron

3.2.1 Effects of temperature on leaching efficiency of iron

Pyrite (FeS_2) is the primary phase in the complex sulfides ore, and it is necessary to figure out the behavior of iron in the leaching process.

Figure 6 shows the effect of temperature on the extraction of iron. The operating conditions are the same as those of antimony leaching process. The operating conditions are 4.0 mol/L HCl, 300 r/min stirring speed, 2.0 L/min gas flow rate, and 50 mL/g L/S ratio. The results indicate that iron extraction increases rapidly from 20.5% to 28.8% with increasing the temperature from 15 to 85 °C. Higher temperature makes the reaction molecules move faster and strengthens the gas–liquid–solid mass transfer, so the leaching efficiency of iron increases with the increase of temperature.

In order to determine the kinetic parameters and rate-controlling step for Fe extraction from complex sulfides ore, the experimental data presented in Fig. 7(a) are analyzed on the basis of the shrinking-core model. The kinetics equation can be obtained through fitting all experimental data with different kinetics models and various rate-controlling mechanisms. The linear relationship between $1-(1-x)^{2/3}$ and leaching time is significant, so it is found that the leaching process is controlled by diffusion in the temperature range of 15–85 °C. To calculate the activation energy, the rate constants are determined and plotted against $1/T$ (Arrhenius plot) as presented in Fig. 7(b). The activation energy of the process is calculated to be 1.99 kJ/mol. The

value of the activation energy clearly indicates that the leaching of Fe from the complex sulfides ore is most likely controlled by diffusion of reactants.

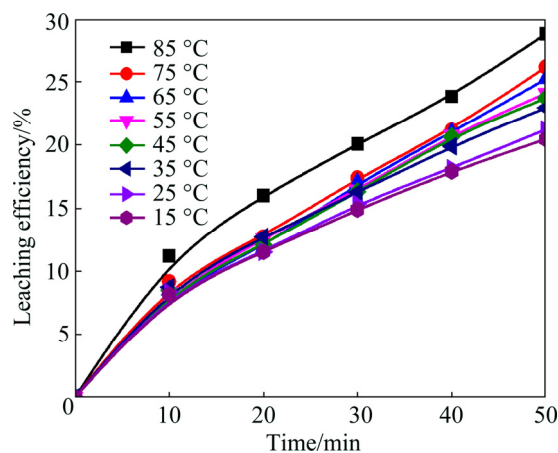


Fig. 6 Effects of temperature on leaching efficiency of iron from antimony-bearing complex sulfides ore

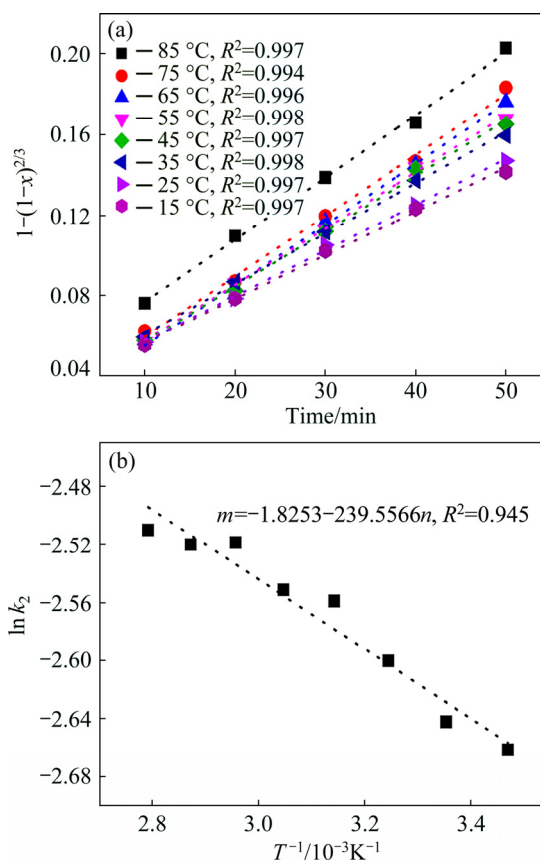


Fig. 7 Plots of $1-(1-x)^{2/3}$ vs time (a) and Arrhenius plot for iron leaching from complex sulfides ore (b)

3.2.2 Effect of acid concentration, stirring speed and particle size and kinetic model

In order to figure out the kinetic model, the effects of acid concentration, stirring speed and particle size were investigated, respectively. The results are shown in Fig. 8.

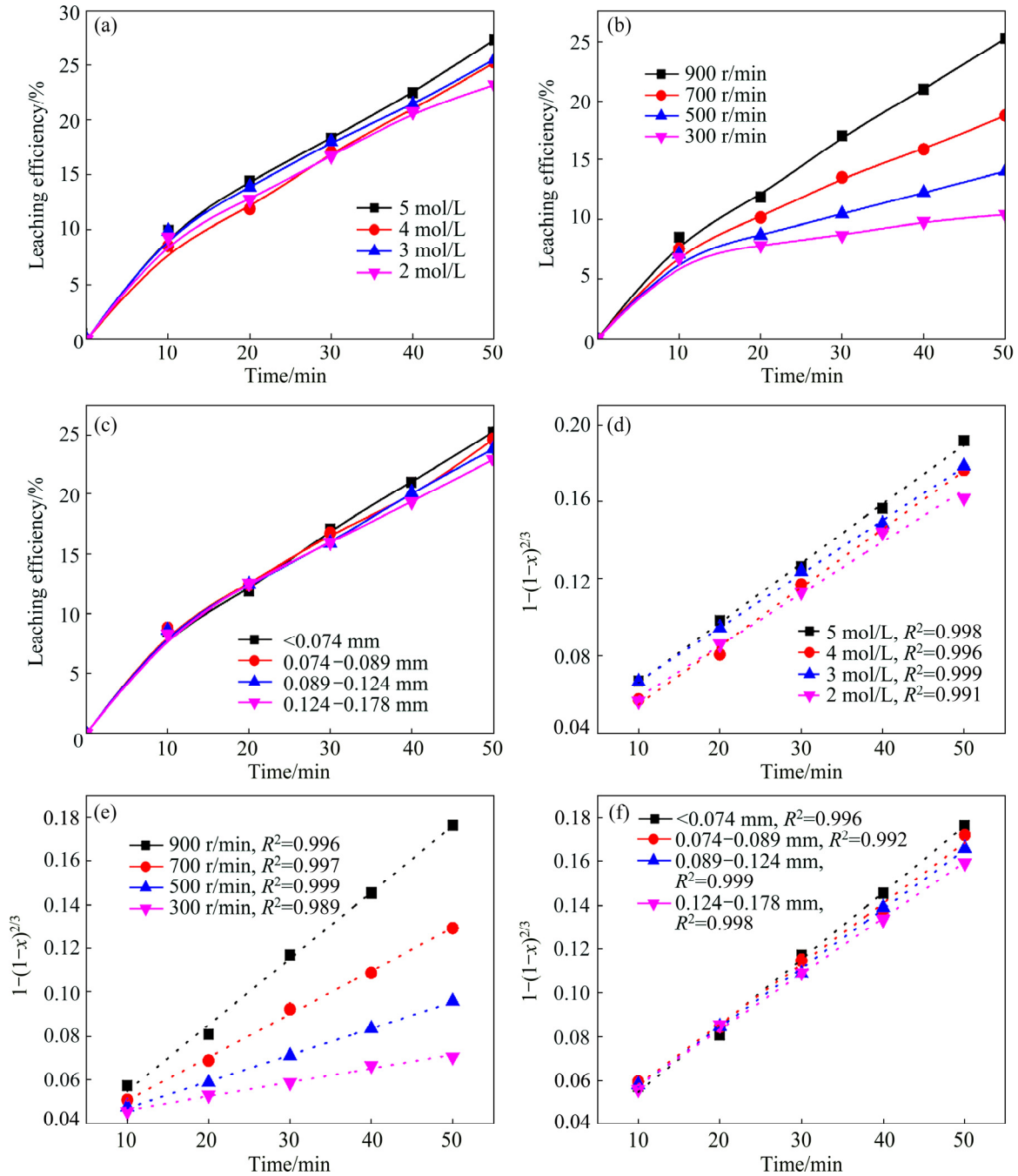


Fig. 8 Leaching efficiency of iron and plots of $1-(1-x)^{2/3}$ vs time

Figure 8(a) shows the result of iron extraction in the HCl concentration range of 2.0–5.0 mol/L with operating conditions: 900 r/min stirring speed, 2.0 L/min gas flow rate, <0.074 mm particle size and 50 mL/g L/S ratio. The extraction of Fe increases slightly from 23.2% to 27.3% with the increase of HCl concentrations from 2.0 to 5.0 mol/L. Different from antimony, the leaching of Fe does not need the complexation of Cl^- , so the higher concentration of HCl does not promote the leaching of Fe significantly. Figure 8(b) shows the results of iron extraction with the stirring speed of 300–900 r/min with

operating conditions: 4.0 mol/L HCl, 2.0 L/min gas flow rate, <0.074 mm particle size and 50 mL/g L/S ratio. The leaching efficiency of Fe increases significantly from 10.4% to 25.3% with the increase of stirring speed. The leaching process is diffusion-controlled from the result above. Stirring speed mainly affects mass transfer, and high stirring speed enhanced the interface behavior of reactants and promoted the reaction rate. Figure 8(c) presents the effects of particle size. The leaching efficiency of iron increases slightly with the decrease of particle size.

The experimental data are fitted according to Eq. (3), and plotted against reaction time, where the correlation coefficient (R^2) is given in Figs. 8(d), (e) and (f). The results show that the leaching process corresponds to diffusion-controlled model well.

The $\ln k$ can be calculated from these k values in Fig. 8(d), (e) and (f). The values of a , b and c in Eq. (7) are determined by linear regression analysis according to $\ln k$, $\ln C$, $\ln S$ and $\ln d$, respectively (Table 3), to be $a=0.1649$, $b=1.4093$ and $c=-0.0005$, so the pre-exponential factor in Eq. (5) becomes

$$A=A_0C^{0.1649}S^{1.4093}d^{-0.0005} \quad (12)$$

Table 3 Fitting results of $\ln k_1$ vs $\ln C$, $\ln S$ and $\ln d$

Factor	Linear equation	R^2
HCl concentration	$m=0.1649n-6.0455$	0.900
Stirring speed	$m=1.4093n-15.4306$	0.993
Particle size	$m=-0.0005n-0.9264$	0.787

The intercept of line in Fig. 7(b) is $\ln A$, and A value is 0.1612. Based on Eq. (12), the value of A_0 is determined to be $8.83 \times 10^{-6} \text{ s}^{-1}$. Above all, we can get the leaching kinetics equation at low temperature:

$$1-(1-x)^{2/3}=8.83 \times 10^{-6} C^{0.1649} S^{1.4093} d^{-0.0005} \exp(-1991.67/(RT))t \quad (13)$$

4 Conclusions

1) Leaching efficiency of antimony increases with increasing temperature, hydrochloric acid concentration, stirring speed and decreasing particle size. However, the HCl concentration and particle size have little effect on the iron dissolution. 86.1% Sb is extracted under the conditions of <0.074 mm particle size, 4.0 mol/L HCl at 85 °C with stirring speed of 900 r/min after 50 min leaching.

2) XRD analysis indicates that no new solid product is formed in the leaching residue particle and the kinetic data are fitted well with shrinking core model.

3) The following kinetic expressions can be used to describe the leaching process of Sb from antimony-bearing complex sulfides ore in HCl solution by ozone:

$$1-(1-x)^{1/3}-k_1/k_2(1-(1-x)^{2/3})=20.95C^{0.6030}S^{0.4405}d^{0.3892}\exp(-17931.75/(RT))t, \quad 45-85 \text{ }^\circ\text{C}$$

$$1-(1-x)^{2/3}=6.19C^{0.6242}S^{0.1937}d^{-0.5957}\exp(-6905.3/(RT))t, \quad 15-45 \text{ }^\circ\text{C}$$

The apparent activation energies of Sb leaching process are 17.93 and 6.91 kJ/mol, respectively. Both the chemical reaction and diffusion of reactants affect the

leaching rate at high temperature, while at low temperature, the leaching rate is controlled by diffusion of reactants.

4) The leaching of Fe corresponds to diffusion-controlled model, and the apparent activation energy is 1.99 kJ/mol. The next kinetic expression can be used to describe the leaching process of Fe:

$$1-(1-x)^{2/3}=8.83 \times 10^{-6} C^{0.1649} S^{1.4093} d^{-0.0005} \exp(-1991.67/(RT))t$$

References

- [1] OORTS K, SMOLDERS E. Ecological threshold concentrations for antimony in water and soil [J]. Environmental Chemistry, 2009, 6: 116–121.
- [2] YANG Xue-ling. Antimony market analysis report in 2013 [J]. Lead-Zinc-Tin and Antimony in China, 2014(1): 45–54. (in Chinese)
- [3] XIE Zhao-feng, YANG Tian-zu, LIU Wei-feng, HUANG Zhen-gao. Study on smelting of Jamesollite without pollution [J]. Mining and Metallurgical Engineering, 2009, 29(4): 80–84. (in Chinese)
- [4] DAI Xi, ZHOU Kang-jie, LI Liang-bin XU Xing-liang. Study on oxygen enriched volatile bath smelting of stibnite concentrate [J]. Mining and Metallurgy, 2015, 24(4): 27–31. (in Chinese)
- [5] WANG Ji-kun, LEI Ting. Treating low grade antimony ore by bath smelting-continuous fuming process [J]. Nonferrous Met, 2000, 52: 44–48. (in Chinese)
- [6] TIAN Qing-hua, JIAO Cui-yan, GUO Xue-yi. Extraction of valuable metals from manganese-silver ore [J]. Hydrometallurgy, 2012, 119: 8–15.
- [7] RASCHMAN P, SMINCAKOVA E. Kinetics of leaching of stibnite by mixed Na_2S and NaOH solutions [J]. Hydrometallurgy, 2012, 113: 60–66.
- [8] UBALDINI S, VEGLIO F, FORNARI P, ABBRUZZESE C. Process flow-sheet for gold and antimony recovery from stibnite [J]. Hydrometallurgy, 2000, 57: 187–199.
- [9] ANDERSON C G. The industrial alkaline sulfide hydrometallurgical treatment of mercury bearing antimony ores and concentrates [C]// San Diego, CA: TMS Annual Meeting, 2003: 227–237.
- [10] ANDERSON C G. The metallurgy of antimony [J]. Chemie der Erde - Geochemistry, 2012, 72(s4): 3–8.
- [11] TIAN Qing-hua, WANG Heng-li, XIN Yun-tao, LI Dong, GUO Xue-yi. Effect of selected parameters on stibnite concentrates leaching by ozone [J]. Hydrometallurgy, 2016, 165: 295–299.
- [12] YANG Jian-guang, WU Yong-tian. A hydrometallurgical process for the separation and recovery of antimony [J]. Hydrometallurgy, 2014, 143: 68–74.
- [13] DU Xin-Ling, TANG Chang-qing. Production technology of high-purity antimony white [J]. Liaoning Chemical Industry, 2007, 36(12): 853–856. (in Chinese).
- [14] Xue-yi GUO, Yun-tao XIN, Hao WANG, Qing-hua TIAN. Study on mineralogical characterization and pre-treatment by ozone of complex refractory gold concentrates [J]. Transactions of Nonferrous Metals Society of China, 2017, 27(8): 1888–1895.
- [15] TIAN Qing-hua, WANG Heng-li, XIN Yun-tao, LI Dong, GUO Xue-yi. Ozonation leaching of a complex sulfidic antimony ore in hydrochloric acid solution [J]. Hydrometallurgy, 2016, 159: 126–131.
- [16] FENG Xing-liang, LONG Zhi-qi, CUI Da-li, WANG Liang-shi, HUANG Xiao-wei, ZHANG Guo-cheng. Kinetics of rare earth leaching from roasted ore of bastnaesite with sulfuric acid [J].

- Transactions of Nonferrous Metals Society of China, 2013, 23(3): 849–854.
- [17] ZHENG Ya-jie, CHEN Kun-kun. Leaching kinetics of selenium from selenium-tellurium-rich materials in sodium sulfite solutions [J]. Transactions of Nonferrous Metals Society of China, 2014, 24(2): 536–543.
- [18] LI Hong-gui. The principles of metallurgy [M]. Beijing: Science Press, 2005: 308–310. (in Chinese)
- [19] TIAN Qing-hua, XIN Yun-tao, YANG Li, WANG Xue-hai, GUO Xue-yi. Theoretical simulation and experimental study of hydrolysis separation of SbCl_3 in complexation–precipitation system [J]. Transactions of Nonferrous Metals Society of China, 2016, 26(10): 2746–2753.

含锑复杂硫化矿在盐酸体系中臭氧氧化浸出动力学

郭学益^{1,2}, 辛云涛^{1,2}, 王浩^{1,2}, 田庆华^{1,2}

1. 中南大学 冶金与环境学院, 长沙 410083;
2. 中国有色金属工业协会 清洁冶金工程研究中心, 长沙 410083

摘要: 开展了复杂硫化矿在盐酸体系中锑和铁的臭氧氧化浸出动力学研究。分别考察温度、HCl浓度、搅拌速度和粒度对反应过程的影响。结果表明: 粒度 <0.074 mm的矿物原料在 $85\text{ }^\circ\text{C}$ 、 4.0 mol/L 盐酸浓度以及 900 r/min 搅拌速度的实验条件下反应 50 min , 可以提取 86.1% 锑和 28.8% 铁。XRD分析表明, 浸出过程并无固体产物生成, 可以认为该反应过程符合收缩核模型。锑的浸出过程在低温($15\sim 45\text{ }^\circ\text{C}$)时为扩散控制, 在高温($45\sim 85\text{ }^\circ\text{C}$)时为混合控制, 反应过程活化能分别为 6.91 和 17.93 kJ/mol ; 铁的浸出过程为扩散过程控制, 活化能为 1.99 kJ/mol ; 最后根据实验结果得出3组动力学方程。

关键词: 臭氧; 含锑难处理硫化矿; 氧化浸出动力学; 混合控制模型; 扩散控制模型

(Edited by Bing YANG)